Source Counts at 90 GHz

M.A. Holdaway, F.N. Owen, M.P. Rupen
National Radio Astronomy Observatory
Socorro, NM 87801

October 31, 1994

1 Abstract

We present the results of sensitive 90 GHz observations by the NRAO 12m of 367 flat spectrum and 51 steep spectrum radio sources. From our sample, we estimate the counts of compact sources suitable for use as MMA calibrators. Over the entire sky, we estimate there are 178 sources with $S_{90} > 1$ Jy and 4400 sources with $S_{90} > 0.1$ Jy. The cores of SSQs make up less than 10% of the compact source counts. The spectral index distribution indicates that there may be enough highly inverted sources to boost the 90 GHz counts above the 30 GHz counts.

2 Introduction

The proposed Millimeter Array (MMA) is designed to work at frequencies as high as 350 GHz on baselines ranging from ~10 m to 3000 m. Extensive site monitoring of the opacity fluctuations at zenith on Mauna Kea and on continental sites (Hogg, 1992)indicate that the atmospheric phase stability on the longest baselines at the highest frequencies will likely be a problem (Holdaway, 1991). We (Holdaway, 1992a; Holdaway, 1992b) and others have proposed a number of calibration schemes to deal with the poor phase stability:

- self-calibration.
- paired antennas, in which adjacent antennas viewing target source and a nearby calibrator.
- phase screen calibration, in which half of the antennas solve for a phase screen using a nearby calibrator source.
- fast switching of all antennas to a nearby calibrator source.
- calculating the phase fluctuations from water vapor column density determined by T_{sys} fluctuations.
- calculating the phase fluctuations from water vapor column density measured by water vapor spectroscopy.
- calculating the phase fluctuations from water vapor column density measured by differential water vapor LIDAR.

In addition to these phase calibration techniques, there are certain tricks we can play to improve the sensitivity of the array, which would improve the performance of the first four calibration techniques which rely on detection of astronomical sources for phase determination:

- burst mode correlation, in which a very wide bandwidth is correlated slower than real time, with the actual observations filling a fraction of the time. Burst mode fits naturally with fast switching.
- phasing subarrays and correlating the reduced number of phased array signals at higher bandwidth than the correlator permits for full array operation.

The success of these calibration schemes can be gauged by the magnitude of the residual phase errors, which will limit the dynamic range of images of the target source. The residual phase errors are estimated as

$$\sqrt{2D_\phi(|\mathbf{v}t + \mathbf{d}|)}, \tag{1}$$

where D_ϕ is the phase structure function, $\mathbf{v}$ is the velocity of the phase screen, t is the time that is required for one cycle of calibration and target source observing, and $\mathbf{d}$ is the distance in the atmosphere between the point the atmospheric phase was determined and the point at which the atmospheric phase is required.

The calibration schemes which do not attempt to measure the atmospheric water vapor directly require a good knowledge of source counts of compact calibrator sources at the calibration frequency in order to determine typical values of t and $\mathbf{d}$. While masers may sometimes be used for calibration purposes in galactic work, the homogeneously distributed extragalactic quasars will usually be used for calibration of most extragalactic observations. To better estimate the source counts of suitable phase calibrators, we have observed 367 flat spectrum quasars (FSQs) and 51 lobe dominated quasars (LDQs) with bright cores with the NRAO 12 m telescope at 90 GHz.

The obvious way to determine the 90 GHz source counts is to perform a complete, sensitive survey of a large enough part of the sky to give us enough sources to determine the all sky source counts to the accuracy we require. Since it is not currently feasible to perform a complete sensitive survey of a large part of the sky at 90 GHz, our search for bright sources at 90 GHz must be guided by complete surveys at other frequencies. The sources which are known to be bright at 90 GHz were discovered because centimeter wavelength surveys indicated they were bright and had flat spectra. This misses the population of sources with highly inverted spectra between centimeter and millimeter wavelengths. Our strategy therefore is to use 90 GHz flux measurements and recent 8.4 GHz flux measurements to derive a distribution of spectral index between 8.4 GHz and 90 GHz ($\psi(\alpha_8^{90})$), which will allow us to transform Condon's (1984) 5 GHz source counts to 90 GHz.

The selection criteria for our sample are given in Section 3. In Section 4 we provide boring details of our observations, while section 5 summarizes the results. In Section 6, we derive estimates for the calibrator source counts at 90 GHz from $\psi(\alpha_8^{90})$ and 5 GHz source counts. Since it is not clear at which frequency the MMA phase calibration should occur, we investigate the source counts at 30 GHz in Section 7. And in Section 8, we indicate the follow-up work we plan to pursue.

3 Source Lists

3.1 Flat Spectrum Sources

Patnaik (1992) has made a VLA 8.4 GHz survey of flat spectrum quasars selected for 5 GHz single dish flux > 200 mJy and spectral index $\alpha < 0.5$ ($S(\nu) \propto \nu^{-\alpha}$) as determined by the GB87 5 GHz source list and the Green Bank 1.4 GHz sky survey maps. The first part of the Patnaik survey includes sources ranging from 35° to 75° declination, and Patnaik has graciously provided us with his source list between 20° and 35°, prior to publication. From Patnaik's survey, we selected about 96 sources in each of four 5 GHz (single dish) flux bins: 200-400 mJy, 400-800 mJy, 800-1600 mJy, and >1600 mJy, taking the

southernmost four sources (one for each flux bin) north of 35° in each hour of right ascension. To obtain 96 sources for the brightest bin required adding flat spectrum sources found in the VLA calibrator list between declination 0° and 75°. Both the Patnaik and the VLA sources have accurate positions.

3.2 Lobe Dominated Sources

We also observed 51 sources from a nonsystematically compiled list of lobe dominated (subjectively defined) radio sources with bright, compact cores at centimeter wavelengths, generally brighter than 100 mJy. These sources were culled from the 3C, Bologna, and other surveys. In this memo, we assume that these lobe dominated sources are steep spectrum sources.

4 Observations

The observations were taken with the NRAO 12 m on November 4–8, 1993. We observed each source for a maximum of three 200 s scans, each scan being made up of 10 double beam switchings to remove the atmospheric contribution to the continuum emission detected at the receivers. The beam size at 90 GHz is 70 arcsec. Telescope pointing was calibrated every 1-3 hours on the planets and on very bright quasars, and a pointing model tied to the telescope's AZ-EL frame with a grid size of roughly 20° was built up for the regions of the AZ-EL space in which we observed most of our sources. The pointing corrections were typically a few arcseconds, though some corrections were as large as five arcseconds. The subreflector was focussed each time the pointing was determined. We used tipping scans to measure the opacity at least once a day, and whenever the monitored opacity at 230 GHz changed sufficiently. The scaling from antenna temperature to flux density was determined from several observations of the planets to be 40.1 Jy/K for channel 1 and 38.2 Jy/K for channel 2.

Three scans, or 600 s of integration, typically resulted in a noise level of 30 mJy RMS. An initial 600 s observation of blank sky gave a signal of 20 mJy. All noise estimates refer to statistical errors, as is relevant to detection experiments. The overall flux scale is probably uncertain to $10-20\%$ If a source was clearly detected ($> 6\sigma$) after one or two scans, we stopped integration at that point. A maximum of three scans was given to any object.

5 Observational Results

The J2000 IAU name, J2000 coordinates, 8.4 GHz flux density, 90 GHz flux density and estimated noise level for the sources in our flat spectrum sample are listed in Table 1. Of the 367 sources observed, 292 were detected at or above the 3σ level. Of the sources in our >1600 mJy bin, 37 were common to Tom Balonek's list of bright quasars, which were observed by him on Nov 26-27, 1993. Rather than reobserving these sources, we have taken Balonek's values for the fluxes. They can be identified in the Table by the round value of 200 mJy for the RMS noise; the sources we observed have lower noise levels.

Table 2 contains the same information for the lobe dominated radio sources with bright centimeter cores. Of the 51 lobe dominated sources with bright cores which we observed, 36 were detected at or above the 3σ level.

6 Compact Source Counts at 90 GHz

Condon's (1984) differential extragalactic source counts at 5 GHz $N_5(S)$ were mainly derived from NRAO 300 ft single dish measurements with a 3′ beam, which includes emission from both a compact

component and steep spectrum extended emission. Given the core fraction distribution at $\nu_\circ$ $\phi(f_c)$ (when not indicated, f_c will stand for the core fraction at 5 GHz), and assuming the core fraction distribution is independent of source strength, the compact core counts at $\nu_\circ$ $M_{\nu_\circ}$ become

$$M_{\nu_\circ}(S) = \int_0^1 df_c N_{\nu_\circ}(S/f_c)\phi(f_c). \tag{2}$$

Given the spectral index distribution $\psi(\alpha)$ ($S \propto \nu^{-\alpha}$) of the cores, with $\psi(\alpha)$ independent of S, the compact source counts at frequency ν are given by

$$M_\nu(S) = \int d\alpha M_{\nu_\circ}(S(\nu/\nu_\circ)^\alpha)(\nu/\nu_\circ)^{-\alpha}\psi(\alpha). \tag{3}$$

We consider the contributions from both flat spectrum, core dominated quasars and steep spectrum, lobe dominated radio sources. These two classes of objects have very different core fraction distributions $\phi(f_c)$, fairly different source counts $N_5(S)$, and may have different spectral index distributions $\psi(\alpha)$, so we treat the flat and steep spectrum sources independently and sum their contributions to obtain the total 90 GHz calibrator source count estimate. We present the details of the derivations of $\psi(\alpha)$ and $\phi(f_c)$ for the FSQ and SSQ populations below. Figure 1 shows the integrated 90 GHz FSQ, SSQ, and total source count estimates we derive. These integrated source counts are appropriate for determining the number of calibrators on the sky brighter than some minimum flux determined by an instrument's sensitivity. The SSQ cores account for only about 8.6% of the potential calibrator sources at 90 GHz at the 100 mJy level, and only 7% at the 200 mJy level.

6.1 Flat Spectrum Quasar Core Source Counts

FSQ Core Spectral Index Distribution $\psi(\alpha)$

The most direct method for estimating $\psi(\alpha)$ is to combine our 90 GHz with Condon's (1984) 5 GHz data. Since both are single-dish surveys, the measured flux densities represent combinations of extended and compact (core) emission, with the relative contribution from each component varying from source to source. This is a problem, because we know that cores have much flatter spectra than extended emission: 5 GHz measurements are more sensitive to extended stuff, while 90 GHz flux densities are generally dominated by compact cores. Fortunately, the 8.4 GHz measurements of Patnaik *et al.* 1992 were made with the VLA in its A configuration, allowing that group to estimate the flux densities of both the compact (0.″2) and the extended (up to 7″) emission. Hence, we can derive a core spectral index from Patnaik's 8.4 GHz core flux and our (core-dominated) 90 GHz single dish fluxes. We further assume that $\psi(\alpha_5^{90})$ can be approximated by $\psi(\alpha_{8.4}^{90})$.

Because the sources we observed cover a wide range of S_{5GHz} (ranging from 0.2 Jy to 35 Jy), our observations allow us to determine whether $\psi(\alpha_{8.4}^{90})$ depends upon $S_{5\mathrm{GHz}}$. Since a fair fraction of the sources in the weaker two S_{5GHz} bins were not detected, we must use the information in the nondetections. We have taken the spectral index distribution from one of the brighter two bins, in which almost all sources were detected at 90 GHz, performed Monte-Carlo simulations of 90 GHz observations of the weaker bins, and then asked if the Monte-Carlo simulations were significantly different from the 90 GHz data in one of the weak bins. The data and the simulations are consistent, so there is no evidence that the spectral index distribution depends on 5 GHz source strength. The spectral index distribution derived from the two brighter 5 GHz bins was used in the FSQ compact source counts, and is shown in Figure 2; it is approximately Gaussian with a peak value of 0.368 and a dispersion of 0.34.

FSQ Core Fraction Distribution $\phi(f_c)$

We determined $\phi(f_c)$ in two different ways:

- Assume the (unknown) core spectral index distribution between 5 GHz and 90 GHz $\psi(\alpha_5^{90})$ is equal to that measured between 8.4 GHz and 90 GHz $\psi(\alpha_{8.4}^{90})$. Then any differences between the core spectral index distribution and the pseudo-spectral index distribution between the 90 GHz core flux and the 5 GHz total flux is due to $\phi(f_c)$ and variability. A simple analysis shows that the two spectral index distributions may be reconciled if the mean core fraction at 5 GHz is 0.8 with a dispersion of about 0.2, independent of S_{5GHz}. Reducing the 5 GHz fluxes by 0.8 will reduce the number of sources brighter than S by $0.8^{-3/2}$, or 1.4. Using this core fraction distribution leads to inconsistencies between the estimated 90 GHz source counts and the numbers of sources known to be bright at 90 GHz.

- Assume the distribution of core fractions at 5 GHz is the same as that determined by comparing Patnaik's core and total fluxes at 8 GHz. (The total fluxes were courteously provided by Patnaik, although they were not published in Pataik *et al.* 1992.) The drawback to this method is that Patnaik's images are not sensitive to features larger than about 7″, so his total power is a lower limit, biasing our core fraction distribution estimate towards larger values.

Taking a 5 GHz core fraction of 0.8 leads to FSQ counts which are significantly belows the number of already-known bright sources at 90 GHz. Since we were unable to rationalize away the known bright sources or otherwise increase our 90 GHz source count estimates, we have used the core fraction distribution derived from Patnaik's data when calculating the FSQ counts. This FSQ core fraction distribution is shown in Figure 3.

Justification for FSQ Core Fraction Distribution

We have two very different choices for the FSQ core fraction distribution which lead to very different estimates of the 90 GHz source counts. In this section we justify our choice of the core fraction distribution derived from Patnaik's (1992) data.

Liszt (1994) has assembled a list of extragalactic sources brighter than 0.5 Jy, along with fairly current fluxes as determined at various observatories. The counts in this list indicate that it is quite incomplete at the 0.5 Jy level, so we focus on the brighter sources; there are 113 FSQs with $S_{90GHz} \geq 1$ Jy north of $\delta = -30°$ in this list. Our work in November 1993 provided 6 more sources with $S_{90GHz} \geq 1$ Jy, and preliminary results from our limited time in October 1994 indicate we have found 10 more sources with $S_{90GHz} \geq 1$ Jy, while we expect to find about 30 more north of $\delta = -30°$. Over all the sky, there should be $\geq$ 216 such sources. The 90 GHz source count estimates made by using a simple 0.8 core fraction predict only 116 sources brighter than $S_{90GHz} \geq 1$ Jy over 4π steradians. What could lead to this discrepancy?

- *Some of the "known" bright sources in Liszt's list may be much weaker at the present epoch.* In April 1994, there were 66 sources brighter than 1 Jy in Balonek's list, 16 1 Jy sources which we have found or measured in the last year, and 30 1 Jy sources which we expect to detect shortly, or *at least* 150 sources all sky (there are many known bright sources which are not in Balonek's list), which is inconsistent with the 116 estimated using the 0.8 core fraction for FSQs.

- *Some FSQ may be hiding as SSQ in Condon (1984).* For example, if a core dominated source were flaring during the 1.4 GHz survey but quiescent when the 5 GHz flux was measured, it would be classified as a steep spectrum object in spite of the fact that it is core dominated and may have a

bright component at 90 GHz. We have investigated a 400 square degree region of the sky defined by $17h < \alpha < 19h$ and $22° < \delta < 38°$. The primary reason for choosing this region was that it contained sensitive 4.85 GHz surveys at three different epochs. We took source data from six different surveys available through ADS: the B2 (408 MHz), Texas (365 MHz), White and Becker (WB92) (GB 1.4 GHz), MIT GB2 (4.85 GHz), MIT GB3 (4.85 GHz), and GB 1987 (4.85 GHz) surveys. We had little trouble finding positional matches among the surveys for sources above 200 mJy in WB92. We determined which sources would be considered flat spectrum from the White and Becker and the GB 87 lists (as did Patnaik), and further asked which sources display evidence of being core dominant in the other surveys. Core dominated sources would be time variable in the three different 4.85 GHz surveys, and a self-absorbed flat spectrum core dominated source would give a poor fit to a power law in frequency while a lobe dominated source with optically thin synchrotron emission would have a spectrum which is well fit by a power law. This investigation produced a few clear examples of core dominated sources masquerading as steep spectrum quasars as judged by the GB87-WB92 comparison, but this would only raise the core dominated source counts by about 10%, which is not enough to produce estimated 90 GHz source counts which are consistent with the number of known bright sources at 90 GHz.

- *We may be underestimating the inverted spectrum tail of $\psi(\alpha)$.* Our 90 GHz observations indicate that $\sim$ 15% of the sources have inverted spectra between 8.4 and 90 GHz. The details of the inverted tail of the spectral index distribution are very important, since this tail allows a small fraction of the much more numerous weaker sources to be boosted up to bright sources at 90 GHz. The inverted tail of our estimated spectral index distribution may be inaccurate since it is determined by only a few sources, and the source counts we derive could be wrong. However, for this to explain the excess known sources, many of the known sources would need to be drawn from the population of inverted sources, and most of the known sources have fairly flat or slightly falling spectral index. Indeed, the inverted sources are the very ones which we are detecting.
- *Our software could be wrong.* No, the software reproduces Condon's (1984) analytical answer for source count frequency transformations assuming a source count coefficient which is independent of source flux.
- *The core fraction distribution of the FSQs in not well described by the single value of 0.8.* Using the distribution derived from Patnaik's data yields 175 1 Jy sources at 90 GHz. This is still inconsistent with the 216 known 1 Jy sources at 90 GHz. but is consistent with the $\sim$ 150 sources which we know to be brighter than 1 Jy right now.

Since the source count estimate which results from the 0.8 core fraction is inconsistent with the lower limit of sources already known to be bright at 90 GHz, we have used a core fraction distribution derived from Patnaik's data. However, it seems likely that the resulting source count estimate is still lower than the known bright 90 GHz sources, and should therefore be viewed as a lower limit.

6.2 Steep Spectrum Quasar Core Source Counts

To estimate the contribution of the flat spectrum cores of SSQs to the 90 GHz calibrator counts, we assume:

- the SSQ $\phi(f_c)$ can be estimated from the steep spectrum subsample of the 3CRR sample.
- the SSQ $\phi(f_c)$ is independent of the SSQ $\psi(\alpha)$.
- the SSQ $\psi(\alpha)$ can be represented by the $\psi(\alpha)$ of our lobe dominated sample.

SSQ $\phi(f_c)$ for the 3CRR Sample

Single dish measurements of the 3C sample at 5 GHz were obtained from Kellerman et al (1969). For sources in the 3CRR sample for which no 5 GHz total power was available, the 5 GHz flux was estimated from the spectral index and the total power at the next highest measured frequency. Core fluxes were culled from the literature, notably from Leahy (1985), Baum (1987), and Laing and Owen (in preparation). Most of the core fluxes were measured at 5 GHz, though a few values are from different frequencies. The core fraction distribution for the 3CRR sources is plotted in Figure 3.

SSQ Core Spectral Index Distribution $\psi(\alpha)$

The centimeter core fluxes for the 51 observed lobe dominated sources (which we associate with the SSQs) were gathered from the literature (see Table 2). The measurements were at frequencies ranging from 1.4 GHz to 15 GHz, and were readjusted to 8.4 GHz based on the spectral index between the frequency of the centimeter flux measurement and 90 GHz. Since we detected only 36 of the 51 SSQ cores we observed, we derived the spectral index distribution using the ASURV software package, Revision 1.1 (LaValley, Isobe and Feigelson 1992), which implements the methods presented in Feigelson and Nelson (1985). The spectral index distribution for the lobe dominated quasars is plotted in Figure 2.

Comparing to the FSQ spectral index distribution, it appears that the cores of the SSQs are *more inverted* than the cores of FSQs. This runs counter to what is expected from conventional core emission models and extragalactic radio source unified schemes. If these cores are intrinsically similar with a spectral steepening at some frequency in the rest frame, we expect the less-beamed SSQ (lobe dominated) cores to have steeper spectra than the more beamed FSQ (core dominated) sources. This discrepancy could be explained if a significant fraction of the flux measured at 90 GHz is due to steep spectrum extended emission or hotspots. We are investigating this effect with VLA observations at 8.4 GHz and 43 GHz of part of the 3CRR sample and part of Patnaik's sample of FSQs.

7 Source Counts at 30 GHz

The MMA is designed to cover all of the transparent windows between 30 GHz and 350 GHz. It is possible to observe a calibrator at one frequency and scale the atmospheric phases to the frequency of the target observations. For this to work, we must know the total water vapor path lengths through the atmosphere, not just the relative phases; this requires observations at multiple frequencies. Typical good conditions at the high mountain sites under investigation for the MMA site have about 1 mm of water vapor, resulting in ~5 turns of phase at 230 GHz, 2 turns at 90 GHz, 0.87 turns at 40 GHz, and 0.65 turns at 30 GHz. (The phase difference between two antennas is usually a small fraction of this.) Monitoring a calibrator at 30 GHz and 40 GHz should allow us to determine the absolute phase and the wrap, and therefore the path length, which would then determine the phase at the frequency of the target observations.

To first order, the system temperature between 30 GHz and 350 GHz increases linearly with the frequency. However, if the phase is determined at a low frequency and applied to observations at the high frequency, the SNR of those calibration observations will need to be better by the ratio of the frequencies, cancelling any advantage due to the improvement in system temperature. Minor sensitivity improvements are made at the lower frequency due to improved aperture efficiency and atmospheric transparency. Hence, there are no compelling instrumental reasons for calibrating at 30 GHz[1]. The

[1] If the MMA is upgraded to operate at 410, 650, or 800GHz, the system temperature and the atmospheric opacity conspire to make calibration at any of the lower frequencies much more attractive, and 30 GHz is the best frequency.

main factor which will determine the preferred calibration frequency will be the source counts. While the source counts at 90 GHz are made up of flat spectrum quasars and cores of steep spectrum quasars, the 30 GHz source counts will have an extra contribution from compact steep spectrum objects. For the time being, we will ignore the compact steep spectrum source counts since reliable fluxes for these sources at 30 GHz are not available.

First, we present an analytical argument for source counts at 30 GHz *vs.* 90 GHz. Condon (1984) shows that if the source counts at frequency $\nu_\circ$ follow a power law

$$N(S,\nu_\circ) = k_\circ S^{-\gamma_\circ}, \tag{4}$$

and if the spectral index distribution is a Gaussian independent of source flux

$$\psi(\alpha,\nu_\circ) = \frac{1}{\sqrt{2\pi}\sigma_\circ}\exp\left[-\frac{(\alpha-\bar{\alpha}_\circ)^2}{2\sigma_\circ^2}\right], \tag{5}$$

then the source counts at another frequency ν will also be a power law

$$N(S,\nu) = kS^{-\gamma_\circ} \tag{6}$$

with the density factor k given by

$$k = k_\circ(\nu/\nu_\circ)^q, \tag{7}$$

q being given by

$$q = \bar{\alpha}_\circ(1-\gamma_\circ) + \ln(\nu/\nu_\circ)\sigma_\circ^2(1-\gamma_\circ)^2/2. \tag{8}$$

The spectral index distribution we determined for the flat spectrum quasars can be described by a Gaussian with $\bar{\alpha} = 0.368$ and $\sigma = 0.34$. Then the ratio of the density factors k_{90}/k_{30} is 1.06, implying that there are more sources at 90 GHz than at 30 GHz. This effect is caused by the spread in the spectral index distribution: some fraction of the sources have inverted spectral index, and are brighter at 90 GHz than at 30 GHz. This effect is quite sensitive to the spectral dispersion: if $\sigma = 0.32$, then there are equal numbers of sources at 30 GHz and 90 GHz. If we use the binned spectral index distribution which we measured, not extrapolating to highly inverted sources (see Figure 4), then we find that there are slightly more sources at 30 GHz below 300 mJy, and more sources at 90 GHz above 300 mJy. A better determination of the inverted tail of the spectral index distribution is required for an estimate of the 90 GHz source counts for purposes of comparison with 30 GHz. Furthermore, the above analysis assumes that the spectral index of each source is independent of frequency, which is not correct. Owen *et al.* (1980) have made simultaneous flux measurements of flat spectrum sources at several different frequencies and find that the spectra of many sources peak around 30 GHz and go down at 90 GHz. Steppe (1988) finds that there are no inverted sources between 22 GHz and 90 GHz, but we find 15% of our sources are inverted between 8.4 GHz and 90 GHz. A consistent picture arises if our inverted sources are all due to a population of sources which is highly inverted between 8.4 and 22 GHz and gently falling between 22 GHz and 90 GHz. Such a population of sources would make 30 GHz a better frequency for calibration.

8 Future Work

We have several upcoming observations to attempt to answer many of the questions which arise from the present investigation:

- The inverted spectrum tail of the spectral index distribution is not well determined due to the small number of sources which have inverted spectra. Since small errors in the inverted tail can result in large errors in the estimated source counts, we have begun a survey aimed at detecting sources which are much brighter at 90 GHz than at centimeter wavelengths.
- Since we cannot assume the spectral index between 8.4 GHz and 90 GHz is constant for these sources, we are observing ~100 sources at 22 GHz and 43 GHz with the VLA to allow us to estimate the 30 GHz source counts.
- Using the source counts presented here, we will employ Monte Carlo simulations to determine typical distances between a target source and the nearest calibrator, as a function of minimum calibrator flux.
- We will soon embark upon a campaign of much more realistic phase calibration simulations.

9 Acknowledgements

Alok Patnaik very kindly sent us his published positions and fluxes in machine readable form, together with source information prior to publication. The NRAO 12 m staff made these observations possible by refining their continuum system. We would like to thank the 12 m operators for being so helpful and for putting up with all the source changes. And we would also like to thank Balonek and Dent for their current bright quasar flux measurements which they provide to the 12 m users.

10 References

1. Baum, S., 1987, Thesis.
2. Condon, 1984, ApJ.
3. Feigelson, E.D. and Nelson, P.I. 1985, ApJ **293**, 192.
4. Feigelson, 1992 ASURV
5. Hogg, D., 1992, MMA Memo 78, "A Summary of the Data Obtained During the mmA Site Survey".
6. Holdaway, 1991, MMA Memo 68, "A Millimeter Wavelength Phase Stability Analysis of the South Baldy and Springerville Sites".
7. Holdaway, 1992a, MMA Memo 84, "Possible Phase Calibration Schemes for the MMA".
8. Holdaway, 1992b, MMA Memo 88, "Paired Antenna Phase Calibration: Residual Phase Errors and Configuration Study".
9. Kellerman *et al.*, 1969, ApJ **157**, 1.
10. Laing, R. and Owen, F.N. (in preparation).
11. LaValley, M., Isobe, T. and Feigelson, E.D. 1992, BAAS, "ASURV".
12. Leahy, P. 1985, Thesis.
13. Owen et al, 1980.
14. Patnaik et al, 1992, MNRAS 254, 655.
15. Steppe 1988, A&AS, **75**, 317.

Table 1: Flat Spectrum Quasars

J2000 Name	J2000 RA	J2000 DEC	S_{90} mJy	σ_{90} mJy	$S_{8.4}$ mJy	$\alpha_{8.4}^{90}$ ($S_\nu \propto \nu^{-\alpha}$)
J0005+3820	00:05:57.17550	38:20:15.1685	843	41	1149	0.130
J0009+4001	00:09:04.17497	40:01:46.7245	70	29	188	> 0.324
J0013+4051	00:13:31.13114	40:51:37.1480	723	36	534	-0.127
J0020+4304	00:20:49.97982	43:04:38.3286	33	25	137	> 0.254
J0025+3919	00:25:26.15705	39:19:35.4466	277	28	440	0.195
J0029+3456	00:29:14.24355	34:56:32.2545	222	27	1025	0.645
J0031+5401	00:31:01.75468	54:01:50.5868	35	20	323	> 0.709
J0037+3659	00:37:46.14372	36:59:10.9280	123	28	139	0.051
J0038+4137	00:38:24.84498	41:37:06.0046	276	28	1008	0.546
J0038+5035	00:38:28.41356	50:35:25.8225	87	27	205	0.361
J0042+2320	00:42:04.54830	23:20:01.1562	264	31	888	0.511
J0046+3900	00:46:47.57892	39:00:47.1485	75	23	195	0.402
J0052+4402	00:52:27.82855	44:02:54.5142	111	28	189	0.224
J0100+6808	01:00:51.66449	68:08:20.5466	155	27	855	0.720
J0102+5824	01:02:45.76299	58:24:11.1392	2821	45	1386	-0.299
J0105+4819	01:05:49.92953	48:19:03.1829	124	24	721	0.742
J0108+0135	01:08:38.77100	01:35:00.3200	1500	200	2050	0.131
J0110+6805	01:10:12.86977	68:05:41.2197	235	25	465	0.287
J0112+3522	01:12:12.94503	35:22:19.2954	243	37	372	0.179
J0113+4026	01:13:17.78004	40:26:13.1005	67	29	75	> -0.062
J0113+4948	01:13:27.00695	49:48:24.0572	844	30	491	-0.228
J0119+3210	01:19:34.99912	32:10:50.0129	251	40	1013	0.588
J0132+4325	01:32:44.12727	43:25:32.6667	375	35	214	-0.236
J0136+4751	01:36:58.59530	47:51:29.1020	1700	200	1603	-0.024
J0136+4751	01:36:58.59530	47:51:29.1020	1734	49	1603	-0.033
J0143+4129	01:43:03.18361	41:29:20.4367	209	30	223	0.027
J0148+3854	01:48:24.37679	38:54:05.2227	151	30	311	0.304
J0152+3716	01:52:12.22113	37:16:05.6763	293	32	240	-0.084
J0154+4743	01:54:56.29019	47:43:26.5392	435	53	575	0.117
J0156+3914	01:56:31.40881	39:14:30.9289	370	49	161	-0.350
J0202+4205	02:02:43.65401	42:05:16.3423	186	25	368	0.287
J0204+3649	02:04:55.59586	36:49:18.0007	69	32	264	> 0.426
J0204+1514	02:04:50.41390	15:14:11.0450	1651	59	2320	0.143
J0226+3421	02:26:10.33437	34:21:30.2581	307	33	1225	0.583
J0228+6721	02:28:50.05158	67:21:03.0238	941	52	1694	0.247
J0230+4032	02:30:45.70679	40:32:53.0870	228	33	486	0.319
J0231+1322	02:31:45.89400	13:22:54.7180	290	35	1970	0.807
J0236+3612	02:36:38.28272	36:12:40.2577	55	27	124	> 0.179
J0237+2848	02:37:52.40611	28:48:08.9900	1807	51	3065	0.222
J0238+1636	02:38:38.93010	16:36:59.2760	1475	64	1300	-0.053

Table 1: Flat Spectrum Quasars (Continued)

J2000 Name	J2000 RA	J2000 DEC	S_{90} mJy	σ_{90} mJy	$S_{8.4}$ mJy	α
J0251+4315	02:51:34.53719	43:15:15.8327	207	25	1091	0.700
J0253+3835	02:53:08.88698	38:35:24.9867	327	35	399	0.083
J0254+3931	02:54:42.63160	39:31:34.7140	457	48	365	−0.094
J0257+4338	02:57:59.07693	43:38:37.6777	47	26	113	> 0.156
J0259+4236	02:59:38.38223	42:36:43.1192	11	29	282	> 0.495
J0304+6821	03:04:22.00693	68:21:37.4632	221	30	673	0.469
J0303+4716	03:03:35.24270	47:16:16.2750	800	200	1668	0.309
J0310+3814	03:10:49.88050	38:14:53.8452	596	56	433	−0.134
J0313+4120	03:13:01.96146	41:20:01.1903	779	63	617	−0.098
J0313+3725	03:13:36.27074	37:25:24.1057	62	27	148	> 0.254
J0319+4130	03:19:48.16050	41:30:42.1030	7200	500	33643	0.650
J0321+4359	03:21:36.87080	43:59:22.4808	76	28	261	> 0.478
J0328+3940	03:28:50.31276	39:40:44.5585	31	32	165	> 0.228
J0330+3639	03:30:34.76550	36:39:41.0339	67	23	197	> 0.442
J0336+3218	03:36:30.10760	32:18:29.3430	1318	44	1460	0.043
J0343+3622	03:43:28.95271	36:22:12.4404	144	24	534	0.552
J0349+4609	03:49:18.74250	46:09:59.6621	507	50	683	0.125
J0354+4643	03:54:30.01294	46:43:18.7537	355	32	570	0.199
J0355+3909	03:55:16.59120	39:09:09.8242	140	29	114	−0.086
J0359+6005	03:59:02.64130	60:05:22.0500	558	47	731	0.113
J0359+5057	03:59:29.74770	50:57:50.1610	2400	300	2900	0.079
J0405+3803	04:05:49.26348	38:03:32.2371	148	25	550	0.553
J0414+3418	04:14:37.25718	34:18:51.1376	465	51	1288	0.429
J0419+3955	04:19:22.55018	39:55:28.9766	320	34	617	0.276
J0419+5722	04:19:19.41291	57:22:59.9769	43	36	386	> 0.537
J0420+3849	04:20:13.58588	38:49:43.0439	14	23	134	> 0.279
J0422+5324	04:22:44.40044	53:24:26.2395	245	28	495	0.296
J0423+4150	04:23:56.01039	41:50:02.7020	851	50	1065	0.094
J0427+4133	04:27:46.04549	41:33:01.0910	231	30	562	0.374
J0431+2037	04:31:03.75560	20:37:34.2530	216	30	1660	0.859
J0432+4138	04:32:36.50436	41:38:28.4328	375	30	2227	0.751
J0433+0521	04:33:11.09550	05:21:15.6230	1700	200	3300	0.279
J0440+4244	04:40:07.87198	42:44:40.2509	103	23	246	0.367
J0446+3900	04:46:11.49337	39:00:17.1064	58	21	473	> 0.850
J0449+6332	04:49:23.30971	63:32:09.4532	295	40	423	0.152
J0448+3629	04:48:35.16078	36:29:31.4209	75	23	260	0.524
J0458+5508	04:58:54.84169	55:08:42.0423	205	24	233	0.053
J0502+4746	05:02:25.88525	47:46:04.5393	18	32	136	> 0.146
J0503+0203	05:03:21.19710	02:03:04.6790	215	27	1530	0.827
J0507+4645	05:07:23.65796	46:45:42.3486	216	32	371	0.228

Table 1: Flat Spectrum Quasars (Continued)

J2000 Name	J2000 RA	J2000 DEC	S_{90} mJy	σ_{90} mJy	$S_{8.4}$ mJy	α
J0509+3528	05:09:05.84508	35:28:17.2891	92	28	201	0.329
J0517+4537	05:17:28.89939	45:37:04.8714	156	28	474	0.468
J0518+4730	05:18:12.08986	47:30:55.5360	1	26	378	> 0.665
J0530+1331	05:30:56.41680	13:31:55.1510	4600	200	2480	-0.260
J0532+0732	05:32:38.99710	07:32:43.3010	1532	93	2080	0.128
J0533+4822	05:33:15.86584	48:22:52.8071	1133	61	539	-0.313
J0536+5038	05:36:20.23181	50:38:26.2546	114	21	860	0.852
J0541+5312	05:41:16.17329	53:12:24.8379	161	29	750	0.648
J0541+4729	05:41:49.24487	47:29:07.6028	237	23	541	0.348
J0552+3754	05:52:17.93797	37:54:25.2821	725	26	441	-0.209
J0554+3541	05:54:09.52961	35:41:31.4069	124	27	155	0.094
J0555+3948	05:55:30.80600	39:48:49.1630	1800	200	6974	0.571
J0559+5804	05:59:13.39407	58:04:03.4432	116	29	442	0.564
J0559+3749	05:59:00.45269	37:49:55.5171	41	32	194	> 0.296
J0604+4413	06:04:35.62972	44:13:58.5460	117	33	384	0.501
J0605+4030	06:05:50.85587	40:30:08.1025	283	32	685	0.372
J0614+6046	06:14:23.86660	60:46:21.7540	151	29	746	0.673
J0624+3856	06:24:19.02193	38:56:48.7245	33	26	553	> 0.825
J0625+4440	06:25:18.26517	44:40:01.6284	267	25	175	-0.178
J0633+3612	06:33:14.70324	36:12:07.0182	13	23	123	> 0.243
J0639+3506	06:39:09.58868	35:06:22.5427	32	24	148	> 0.303
J0641+3539	06:41:35.85425	35:39:57.6234	51	26	74	> -0.022
J0642+3509	06:42:58.14017	35:09:18.3876	197	27	173	-0.054
J0644+3914	06:44:53.71000	39:14:47.5407	192	18	574	0.461
J0646+4451	06:46:32.02630	44:51:16.5890	980	49	2177	0.336
J0650+6001	06:50:31.25557	60:01:44.5466	166	25	657	0.580
J0653+3705	06:53:58.28274	37:05:40.6112	510	36	882	0.231
J0655+4100	06:55:10.02429	41:00:10.1479	103	26	330	0.491
J0656+4237	06:56:10.66286	42:37:02.7512	84	23	109	0.109
J0709+3737	07:09:09.22231	37:37:53.1716	21	29	170	> 0.282
J0710+4732	07:10:46.10520	47:32:11.1420	312	25	606	0.279
J0713+4349	07:13:38.16418	43:49:17.1994	148	25	1169	0.871
J0714+3534	07:14:24.81800	35:34:39.7920	93	27	587	0.776
J0717+4538	07:17:51.85314	45:38:03.2521	499	36	518	0.015
J0722+3722	07:22:01.25998	37:22:28.6279	14	31	206	> 0.335
J0730+4049	07:30:51.34725	40:49:50.8263	73	28	335	> 0.583
J0733+5022	07:33:52.52117	50:22:09.0511	538	41	646	0.077
J0738+1742	07:38:07.39380	17:42:19.0000	1300	200	3500	0.417
J0739+0137	07:39:18.03420	01:37:04.6170	1900	200	1680	-0.051
J0741+3112	07:41:10.70368	31:12:00.2259	450	36	3318	0.842

Table 1: Flat Spectrum Quasars (Continued)

J2000 Name	J2000 RA	J2000 DEC	S_{90} mJy	σ_{90} mJy	$S_{8.4}$ mJy	α
J0743+3941	07:43:09.88664	39:41:30.7813	72	31	277	> 0.460
J0745+1011	07:45:33.05950	10:11:12.6930	296	34	2950	0.969
J0750+4814	07:50:20.43759	48:14:53.5603	218	28	625	0.444
J0752+3730	07:52:40.90801	37:30:24.3082	206	26	190	-0.034
J0753+4231	07:53:03.33778	42:31:30.7631	50	26	271	> 0.525
J0753+5352	07:53:01.38500	53:52:59.6370	1221	58	1000	-0.084
J0806+4504	08:06:33.47197	45:04:32.2740	90	28	350	0.572
J0808+4950	08:08:39.66670	49:50:36.5280	1415	51	717	-0.286
J0808+4052	08:08:56.65180	40:52:44.8789	855	55	999	0.065
J0809+3455	08:09:38.88712	34:55:37.2563	24	24	135	> 0.265
J0810+4134	08:10:58.99286	41:34:02.8023	139	34	248	0.244
J0815+3635	08:15:25.94520	36:35:15.1470	305	30	684	0.340
J0818+4222	08:18:16.00000	42:22:45.4120	500	200	1016	> 0.222
J0823+2223	08:23:24.75848	22:23:03.3052	457	49	1170	0.396
J0824+5552	08:24:47.23660	55:52:42.6680	1347	65	1620	0.077
J0824+3916	08:24:55.48368	39:16:41.8978	1473	32	1058	-0.139
J0827+3525	08:27:38.58906	35:25:05.0807	204	26	539	0.409
J0833+4224	08:33:53.88502	42:24:01.8494	359	39	452	0.097
J0834+5534	08:34:54.90264	55:34:21.0855	144	35	2706	1.237
J0836+4125	08:36:36.89322	41:25:54.7062	226	30	256	0.052
J0841+7053	08:41:24.36570	70:53:42.1720	700	200	1692	0.372
J0844+3830	08:44:29.09764	38:30:55.6882	122	27	214	0.237
J0850+3747	08:50:24.73096	37:47:09.4732	222	21	220	-0.003
J0854+5757	08:54:41.99648	57:57:29.9234	139	25	760	0.716
J0854+2006	08:54:48.87518	20:06:30.6393	2600	200	3681	0.146
J0903+4651	09:03:03.99040	46:51:04.1350	364	27	940	0.400
J0903+6757	09:03:53.15590	67:57:22.6827	109	27	600	0.719
J0904+4238	09:04:15.62764	42:38:04.7727	238	27	346	0.157
J0914+3512	09:14:39.42376	35:12:04.5869	94	28	191	0.298
J0916+3854	09:16:48.90469	38:54:28.1421	255	30	422	0.212
J0920+4441	09:20:58.45870	44:41:53.9840	1848	40	1340	-0.135
J0921+6215	09:21:36.23140	62:15:52.1790	965	68	1494	0.184
J0926+4029	09:26:00.42727	40:29:49.6727	123	21	230	0.263
J0927+3902	09:27:03.01420	39:02:20.8500	6100	200	8034	0.116
J0930+3503	09:30:55.27914	35:03:37.6082	724	66	422	-0.227
J0935+3633	09:35:31.84056	36:33:17.5617	110	28	162	0.163
J0945+3534	09:45:38.12074	35:34:55.0776	194	24	254	0.113
J0948+4039	09:48:55.33870	40:39:44.5833	940	36	1220	0.109
J0952+3512	09:52:32.02616	35:12:52.3929	190	28	268	0.145
J0956+3935	09:56:08.55820	39:35:16.1876	154	34	107	-0.153

Table 1: Flat Spectrum Quasars (Continued)

J2000 Name	J2000 RA	J2000 DEC	S_{90} mJy	σ_{90} mJy	$S_{8.4}$ mJy	α
J0957+5522	09:57:38.18251	55:22:57.7336	546	61	1250	0.349
J0958+6533	09:58:47.24520	65:33:54.8150	774	53	1229	0.195
J0958+4725	09:58:19.67008	47:25:07.8314	706	57	768	0.035
J1013+3445	10:13:49.61423	34:45:50.7817	202	23	357	0.240
J1018+3542	10:18:10.98766	35:42:39.4375	245	25	603	0.379
J1020+4320	10:20:27.20211	43:20:56.3419	30	29	131	> 0.172
J1022+4239	10:22:13.13244	42:39:25.6175	142	31	225	0.194
J1023+3948	10:23:11.56580	39:48:15.3840	429	34	752	0.236
J1033+4116	10:33:03.70810	41:16:06.2300	158	28	375	0.364
J1035+5628	10:35:07.03990	56:28:46.7920	29	27	773	> 0.951
J1038+4244	10:38:18.18994	42:44:42.7661	137	22	140	0.009
J1041+5233	10:41:46.77999	52:33:28.2170	365	43	431	0.070
J1042+1203	10:42:44.60600	12:03:31.2590	517	62	1440	0.431
J1051+2119	10:51:48.78950	21:19:52.3485	1092	61	1135	0.016
J1058+0133	10:58:29.60520	01:33:58.8240	1900	200	3750	0.286
J1058+1951	10:58:17.90245	19:51:50.9018	137	25	613	0.631
J1058+4304	10:58:02.92076	43:04:41.5050	181	26	199	0.039
J1101+3904	11:01:30.07043	39:04:32.6207	157	31	225	0.151
J1101+6241	11:01:53.44908	62:41:50.5899	69	29	278	> 0.489
J1104+3812	11:04:27.31462	38:12:31.7875	455	34	538	0.070
J1112+3446	11:12:38.76870	34:46:39.1212	225	32	133	-0.221
J1117+4120	11:17:53.33390	41:20:16.2761	26	24	132	> 0.255
J1130+3815	11:30:53.28220	38:15:18.5526	544	30	748	0.134
J1139+4032	11:39:02.73439	40:32:54.8413	46	24	227	> 0.484
J1146+5848	11:46:26.91199	58:48:34.2423	182	31	522	0.444
J1147+3501	11:47:22.13022	35:01:07.5258	113	25	466	0.597
J1146+3958	11:46:58.29810	39:58:34.3040	827	30	562	-0.162
J1153+4036	11:53:54.65938	40:36:52.6172	128	24	342	0.414
J1158+4825	11:58:26.76904	48:25:16.2350	154	26	382	0.383
J1159+2914	11:59:31.83408	29:14:43.8254	1200	200	1174	-0.009
J1209+4119	12:09:22.78840	41:19:41.3688	214	20	450	0.313
J1215+3448	12:15:55.60197	34:48:15.2135	196	29	686	0.528
J1221+4411	12:21:27.04576	44:11:29.6635	135	24	424	0.482
J1221+2813	12:21:31.69080	28:13:58.4965	300	200	1196	> 0.290
J1223+4611	12:23:39.33646	46:11:18.6041	67	25	141	> 0.266
J1224+4335	12:24:51.50593	43:35:19.2815	138	27	186	0.125
J1225+3914	12:25:50.57029	39:14:22.6806	91	29	330	0.543
J1227+3635	12:27:58.72601	36:35:11.8194	8	20	328	> 0.716
J1229+0203	12:29:06.69970	02:03:08.5980	22989	48	27500	0.075
J1228+3706	12:28:47.42456	37:06:12.0820	112	25	743	0.797

Table 1: Flat Spectrum Quasars (Continued)

J2000 Name	J2000 RA	J2000 DEC	S_{90} mJy	σ_{90} mJy	$S_{8.4}$ mJy	α
J1235+3621	12:35:05.80759	36:21:19.3080	41	23	194	> 0.435
J1236+3920	12:36:51.44906	39:20:27.6937	27	26	152	> 0.281
J1242+3720	12:42:09.81383	37:20:05.6807	67	25	298	> 0.581
J1242+3751	12:42:51.37049	37:51:00.0126	140	28	527	0.558
J1244+4048	12:44:49.18793	40:48:06.1375	46	23	404	> 0.745
J1256-0547	12:56:11.16660	-05:47:21.5270	16960	67	11200	-0.175
J1302+5748	13:02:52.46490	57:48:37.6175	218	27	854	0.575
J1310+3220	13:10:28.66409	32:20:43.7828	2600	200	2956	0.054
J1310+4653	13:10:53.59063	46:53:52.2192	114	21	350	0.473
J1322+3912	13:22:55.66151	39:12:07.9842	32	23	166	> 0.370
J1324+4048	13:24:12.09400	40:48:11.7728	9	22	245	> 0.553
J1326+3154	13:26:16.51370	31:54:09.5170	248	25	1534	0.768
J1327+4326	13:27:20.97896	43:26:27.9969	105	25	448	0.611
J1331+3030	13:31:08.28738	30:30:32.9579	900	200	5121	0.733
J1335+4542	13:35:21.96043	45:42:38.2519	116	20	412	0.534
J1335+5844	13:35:25.92758	58:44:00.2863	176	24	703	0.583
J1337+5501	13:37:49.64084	55:01:02.1208	113	29	541	0.660
J1340+3754	13:40:22.95185	37:54:43.8391	10	23	140	> 0.298
J1347+1217	13:47:33.36040	12:17:24.2010	300	200	2300	> 0.566
J1359+4011	13:59:38.09433	40:11:38.2604	155	27	256	0.211
J1407+2827	14:07:00.39471	28:27:14.6909	4	25	1923	> 1.368
J1415+3706	14:15:28.46657	37:06:21.1789	47	34	240	> 0.360
J1417+4607	14:17:08.16081	46:07:05.4483	213	26	503	0.362
J1419+3821	14:19:46.61407	38:21:48.4841	616	52	678	0.040
J1420+3721	14:20:00.34071	37:21:34.6723	125	24	128	0.01
J1419+5423	14:19:46.59750	54:23:14.7870	800	200	2182	0.423
J1423+4802	14:23:06.15619	48:02:10.8466	57	28	344	> 0.594
J1426+3625	14:26:37.08764	36:25:09.5858	343	31	502	0.160
J1429+5406	14:29:21.87958	54:06:11.1266	160	25	462	0.447
J1430+3649	14:30:40.58347	36:49:03.8951	226	28	257	0.054
J1436+6336	14:36:45.80250	63:36:37.8680	176	36	855	0.666
J1438+3710	14:38:53.61102	37:10:35.4244	88	27	276	0.482
J1458+3720	14:58:44.79492	37:20:21.6266	325	32	334	0.011
J1500+4751	15:00:48.65431	47:51:15.5259	180	23	642	0.536
J1506+3730	15:06:09.53020	37:30:51.1310	688	39	1014	0.163
J1506+4239	15:06:53.04195	42:39:23.0400	579	25	359	-0.201
J1521+4336	15:21:49.61404	43:36:39.2661	426	33	476	0.046
J1534+4823	15:34:04.87272	48:23:40.9059	80	31	65	> -0.151
J1545+4751	15:45:08.53027	47:51:54.6667	1	33	312	> 0.484
J1545+3941	15:45:53.23312	39:41:46.8573	44	26	76	> -0.010

Table 1: Flat Spectrum Quasars (Continued)

J2000 Name	J2000 RA	J2000 DEC	S_{90} mJy	σ_{90} mJy	$S_{8.4}$ mJy	α
J1547+4937	15:47:21.13841	49:37:05.8100	73	27	279	> 0.521
J1549+0237	15:49:29.43710	02:37:01.1640	2100	200	1080	-0.280
J1557+4522	15:57:19.00033	45:22:21.5368	80	27	112	> 0.136
J1602+3326	16:02:07.26391	33:26:53.0812	488	29	2219	0.638
J1608+1029	16:08:46.20350	10:29:07.7760	630	47	1200	0.271
J1613+3412	16:13:41.06447	34:12:47.9098	2600	200	3182	0.085
J1616+3621	16:16:55.58038	36:21:34.5039	46	26	229	> 0.454
J1618+3632	16:18:23.58064	36:32:01.8051	30	28	79	> -0.025
J1620+4901	16:20:31.22632	49:01:53.2537	202	25	349	0.230
J1625+4134	16:25:57.66994	41:34:40.6356	227	27	982	0.617
J1631+4927	16:31:16.54118	49:27:39.5032	481	41	565	0.067
J1632+3547	16:32:31.25781	35:47:37.7395	103	36	157	> 0.157
J1635+3808	16:35:15.49320	38:08:04.5020	2300	200	2412	0.020
J1637+4717	16:37:45.13069	47:17:33.8364	636	46	704	0.042
J1638+5720	16:38:13.45650	57:20:23.9810	1242	60	1304	0.020
J1640+3946	16:40:29.63317	39:46:46.0280	598	46	1649	0.427
J1639+5357	16:39:39.84349	53:57:47.1166	121	27	279	0.352
J1642+3948	16:42:58.81020	39:48:36.9950	700	200	5228	0.847
J1642+6856	16:42:07.84860	68:56:39.7580	700	200	1182	0.220
J1647+3752	16:47:25.74468	37:52:18.0528	16	24	122	> 0.222
J1646+4059	16:46:56.85906	40:59:17.1742	512	54	337	-0.176
J1653+3945	16:53:52.21705	39:45:36.6111	551	39	1094	0.289
J1658+0515	16:58:33.44720	05:15:16.4450	200	200	920	> 0.180
J1658+4737	16:58:02.77937	47:37:49.2445	716	47	1069	0.169
J1657+4808	16:57:46.87882	48:08:33.0519	416	47	624	0.171
J1657+5705	16:57:20.70951	57:05:53.5053	159	27	451	0.439
J1707+3536	17:07:17.75383	35:36:10.5622	37	30	276	> 0.472
J1721+3542	17:21:09.49097	35:42:16.0669	367	32	506	0.135
J1724+4004	17:24:05.42882	40:04:36.4605	393	34	256	-0.180
J1727+4530	17:27:27.65082	45:30:39.7339	690	58	1248	0.249
J1728+3838	17:28:59.14169	38:38:26.4566	172	28	172	0.000
J1734+3857	17:34:20.57880	38:57:51.4450	608	49	1172	0.276
J1735+3616	17:35:48.08683	36:16:45.6099	458	39	887	0.278
J1735+5049	17:35:49.00520	50:49:11.5718	232	26	719	0.476
J1739+4737	17:39:57.12950	47:37:58.3650	343	40	828	0.371
J1740+5211	17:40:36.97810	52:11:43.4090	947	38	1300	0.133
J1743+3747	17:43:47.64647	37:47:53.8260	84	27	363	0.617
J1744+4014	17:44:25.09586	40:14:48.1481	58	26	241	> 0.475
J1751+0939	17:51:32.81850	09:39:00.7280	3900	200	2000	-0.281
J1753+4409	17:53:22.64957	44:09:45.6742	251	30	714	0.440

Table 1: Flat Spectrum Quasars (Continued)

J2000 Name	J2000 RA	J2000 DEC	S_{90} mJy	σ_{90} mJy	$S_{8.4}$ mJy	α
J1754+3540	17:54:13.67609	35:40:48.5488	77	28	117	> 0.139
J1800+3848	18:00:24.76501	38:48:30.6953	457	53	1058	0.354
J1801+4404	18:01:32.31493	44:04:21.9033	655	51	452	-0.156
J1802+4557	18:02:25.14270	45:57:34.6445	84	24	128	0.177
J1806+6949	18:06:50.68070	69:49:28.1100	1300	200	1533	0.069
J1814+4113	18:14:22.70825	41:13:05.6054	145	33	276	0.271
J1821+3945	18:21:59.69913	39:45:59.6472	211	28	228	0.032
J1824+5651	18:24:07.06850	56:51:01.4930	2797	41	1158	-0.371
J1829+3957	18:29:56.52027	39:57:34.6902	52	25	206	> 0.426
J1840+3900	18:40:57.15500	39:00:45.7119	43	30	215	> 0.367
J1840+4042	18:40:44.99744	40:42:36.9268	33	34	57	> -0.245
J1842+6809	18:42:33.64170	68:09:25.2300	378	45	835	0.334
J1849+6705	18:49:16.07136	67:05:41.6786	983	49	422	-0.356
J1852+4019	18:52:30.37400	40:19:06.6006	105	19	506	0.663
J1855+3742	18:55:27.70568	37:42:56.9859	42	34	197	> 0.277
J1902+3159	19:02:55.93492	31:59:41.6383	808	37	1685	0.309
J1912+3740	19:12:25.12308	37:40:36.6587	331	27	302	-0.038
J1925+2106	19:25:59.60580	21:06:26.1663	993	48	1504	0.175
J1936+3642	19:36:27.81691	36:42:34.9884	107	34	400	0.556
J1937+3607	19:37:31.43666	36:07:35.8464	72	29	190	> 0.329
J1939+3817	19:39:33.56628	38:17:35.3974	29	24	147	> 0.301
J1939+3713	19:39:51.80643	37:13:30.4983	109	23	334	0.472
J1944+5448	19:44:31.51376	54:48:07.0685	115	26	607	0.701
J1948+3556	19:48:04.51999	35:56:20.6742	229	33	239	0.018
J1948+3942	19:48:39.87669	39:42:36.4740	29	31	115	> 0.089
J1953+3537	19:53:30.87589	35:37:59.3678	148	26	561	0.561
J1955+5131	19:55:42.73860	51:31:48.5480	1207	56	1738	0.153
J2001+4352	20:01:12.87394	43:52:52.8439	124	27	212	0.226
J2002+4725	20:02:10.41825	47:25:28.7767	230	25	738	0.491
J2002+4506	20:02:52.09662	45:06:08.3391	322	36	487	0.174
J2007+4029	20:07:44.94510	40:29:48.6100	1100	200	2850	0.401
J2006+6424	20:06:17.69491	64:24:45.4226	578	41	851	0.163
J2007+6607	20:07:28.77132	66:07:22.5398	148	22	436	0.455
J2012+4628	20:12:05.63735	46:28:55.7873	597	45	491	-0.082
J2015+4628	20:15:39.98647	46:28:50.8855	58	24	124	> 0.229
J2015+6554	20:15:55.36830	65:54:52.6621	235	31	548	0.357
J2023+3153	20:23:19.01769	31:53:02.3066	1237	43	3295	0.413
J2022+6136	20:22:06.68200	61:36:58.8060	700	200	2933	0.604
J2023+5427	20:23:55.84473	54:27:35.8403	528	44	922	0.235
J2025+3343	20:25:10.83500	33:43:00.1860	1416	47	2900	0.302

Table 1: Flat Spectrum Quasars (Continued)

J2000 Name	J2000 RA	J2000 DEC	S_{90} mJy	σ_{90} mJy	$S_{8.4}$ mJy	α
J2031+5455	20:31:47.95897	54:55:03.1515	215	23	663	0.474
J2038+5119	20:38:37.03510	51:19:12.6650	1900	200	4213	0.335
J2050+3619	20:50:02.28477	36:19:52.5002	425	23	247	−0.228
J2052+3635	20:52:52.05744	36:35:35.2992	73	21	1846	1.362
J2055+6122	20:55:38.83705	61:22:00.6411	233	37	278	0.074
J2109+3532	21:09:31.87845	35:32:57.6023	814	40	829	0.007
J2114+3742	21:14:44.12296	37:42:25.7191	43	21	93	> 0.164
J2120+4434	21:20:31.77341	44:34:34.2810	363	29	302	−0.077
J2123+0535	21:23:44.51740	05:35:22.0950	700	200	2750	0.576
J2125+6423	21:25:27.44899	64:23:39.3488	95	24	987	0.987
J2134+4050	21:34:24.10533	40:50:11.3445	70	29	134	> 0.182
J2136+0041	21:36:38.58640	00:41:54.2150	2000	200	7030	0.530
J2140+3911	21:40:16.94765	39:11:44.8513	94	27	364	0.570
J2148+0657	21:48:05.45870	06:57:38.6060	5100	200	6600	0.108
J2153+4322	21:53:50.95852	43:22:54.4967	35	21	146	> 0.354
J2201+5048	22:01:43.53939	50:48:56.3932	311	30	762	0.377
J2202+4216	22:02:43.29180	42:16:39.9820	1400	200	3215	0.350
J2203+3145	22:03:14.97618	31:45:38.2726	900	200	3172	0.531
J2204+3632	22:04:21.09972	36:32:37.0944	197	21	272	0.136
J2207+3913	22:07:46.07195	39:13:50.3526	33	26	104	> 0.121
J2209+3742	22:09:21.42350	37:42:18.2303	147	24	551	0.557
J2209+5158	22:09:21.48996	51:58:01.8270	71	25	396	> 0.701
J2216+3518	22:16:20.01079	35:18:14.1787	316	47	536	0.222
J2218+4146	22:18:12.23068	41:46:33.5343	146	35	83	−0.238
J2232+1143	22:32:36.40890	11:43:50.9060	2200	200	2750	0.094
J2236+2828	22:36:22.47124	28:28:57.4159	700	200	2045	0.452
J2241+4120	22:41:07.20544	41:20:11.6178	260	21	783	0.464
J2246+3601	22:46:10.86432	36:01:55.6730	35	27	159	> 0.284
J2248+3718	22:48:37.91101	37:18:12.4680	24	22	287	> 0.619
J2250+5550	22:50:42.84959	55:50:14.6079	155	26	381	0.379
J2251+4030	22:51:59.77149	40:30:58.1551	144	28	122	−0.069
J2253+1608	22:53:57.74790	16:08:53.5630	7552	655	10900	0.154
J2255+4202	22:55:36.70820	42:02:52.5350	150	24	693	0.645
J2257+4154	22:57:22.07215	41:54:16.5165	170	23	751	0.626
J2301+3726	23:01:27.73664	37:26:49.2445	247	26	354	0.151
J2322+5057	23:22:25.98310	50:57:51.9649	738	43	1552	0.313
J2330+4104	23:30:08.86744	41:04:25.0841	42	21	77	> 0.084
J2331+4522	23:31:48.96619	45:22:48.9963	45	24	94	> 0.112
J2333+3901	23:33:02.53305	39:01:12.0185	65	25	307	> 0.594
J2346+0930	23:46:36.83890	09:30:45.5180	526	53	1150	0.329

Table 1: Flat Spectrum Quasars (Continued)

J2000 Name	J2000 RA	J2000 DEC	S_{90} mJy	σ_{90} mJy	$S_{8.4}$ mJy	α
J2347+4310	23:47:22.87341	43:10:53.2365	92	23	205	0.337
J2349+3849	23:49:20.82620	38:49:17.5725	674	55	224	−0.464
J2354+4553	23:54:21.67973	45:53:04.2397	582	36	831	0.150
J2355+4950	23:55:09.45870	49:50:08.3420	171	25	922	0.710
J2359+3850	23:59:33.18089	38:50:42.3217	82	28	262	> 0.479
J2358+3922	23:58:59.85538	39:22:28.3103	259	31	293	0.052
J0000+4054	00:00:53.08153	40:54:01.8058	27	30	346	> 0.567

Table 2: Lobe Dominated Quasars

Name	B1950 RA	B1950 DEC	S_{90} mJy	σ_{90} mJy	S_{cm} mJy	Freq GHz	α_ν^{90} ($S_\nu \propto \nu^{-\alpha}$)	Ref
3C47	01 33 40.4	20 42 11	4	25	74	5.0	> -0.005	20
0137+01	01 37 22.9	01 16 36	188	27	232	1.4	0.050	16
0206+35	02 06 39.3	35 33 42	99	27	93	1.4	-0.015	1
0212+17	02 11 59.8	17 08 53	16	27	211	1.4	> 0.265	16
3C66B	02 20 01.7	42 45 55	215	24	230	5.0	0.023	9
3C75	02 55 03.0	05 49 30	56	32	39	5.0	> -0.226	7
IC310	03 13 22.3	41 07 46	-2	16	150	1.4	> 0.167	19
NGC1265	03 14 56.8	41 40 30	58	17	20	4.9	> -0.430	10
0331+39	03 31 01.0	39 11 24	111	26	174	1.4	0.108	1
3C109	04 10 55.0	11 04 41	194	23	219	4.9	0.042	7
3C123	04 33 55.2	29 34 12	692	46	120	15.0	-0.978	12
3C133	04 59 54.3	25 12 12	634	44	250	5.0	-0.322	13
0610+26	06 10 43.7	26 05 31	127	29	500	5.0	0.474	21
0705+48	07 05 21.4	48 41 48	58	16	200	1.4	> 0.252	4
0723+67	07 23 04.3	67 54 53	364	33	408	5.0	0.039	17
0755+37	07 55 09.1	37 55 22	161	27	189	1.46	0.039	2
0821+62	08 21 22.9	62 07 16	255	26	310	5.0	0.068	17
0836+29	08 36 13.5	29 01 13	94	26	125	1.45	0.069	5
3C207	08 38 01.7	13 23 05	510	61	510	5.0	0.000	14
0850+58	08 50 50.2	58 08 56	123	26	607	1.4	0.383	16
3C212	08 55 55.6	14 21 24	105	26	210	15.0	0.387	13
HYDRAA	09 15 41.5	-11 53 09	433	37	230	5.0	-0.219	18
0932+02	09 32 42.9	02 17 41	86	26	103	1.4	0.043	16
1007+41	10 07 26.1	41 47 26	50	29	134	5.0	> 0.225	17
1028+31	10 28 09.9	31 18 21	82	31	148	1.45	0.143	6
3C249.1	11 00 27.4	77 15 09	86	26	110	5.0	0.085	14
1104+16	11 04 36.6	16 44 17	78	30	248	1.4	0.278	16
3C263	11 37 09.3	66 04 27	159	42	130	5.0	-0.070	14
3C264	11 42 29.5	19 53 02	236	28	260	4.9	0.033	7
1150+49	11 50 48.0	49 47 51	1871	25	416	5.0	-0.520	17
3C270.1	12 18 03.9	33 59 51	36	30	192	5.0	> 0.349	15
3C275.1	12 41 27.5	16 39 18	184	32	135	5.0	-0.107	15
1317+52	13 17 41.2	52 03 50	146	32	343	1.4	0.205	16
1347+53	13 47 42.6	53 56 09	97	41	797	5.0	0.729	17
1346+26	13 46 34.1	26 50 29	14	31	726	1.45	> 0.567	6
1423+24	14 23 34.6	24 17 32	69	28	213	1.4	> 0.267	16
1511+26	15 11 30.8	26 18 40	-12	36	317	1.42	> 0.364	3
3C317	15 14 17.0	07 12 19	128	29	232	4.9	0.204	7
1548+11	15 48 21.2	11 29 49	80	22	154	1.4	0.157	16
1618+17	16 18 07.3	17 43 31	81	28	166	1.4	0.172	16

Table 2: Lobe Dominated Quasars (Continued)

Name	B1950 RA	B1950 DEC	S_{90} mJy	σ_{90} mJy	S_{cm} mJy	Freq GHz	Spectral Index	Ref
3C338	16 26 55.3	39 39 37	56	20	105	4.9	> 0.139	8
3C351	17 04 03.5	60 48 32	87	25	620	5.0	0.679	13
1741+27	17 41 57.9	27 54 05	471	50	397	1.4	-0.041	16
1830+28	18 30 52.4	28 31 18	311	29	322	1.4	0.008	16
3C388	18 42 35.5	45 30 22	177	22	100	5.0	-0.198	14
3C390.3	18 45 37.6	79 43 07	382	30	350	5.0	-0.030	7
1924+50	19 24 48.9	50 46 53	115	25	314	5.0	0.348	17
1951+49	19 51 12.1	49 50 25	40	26	91	5.0	> 0.091	17
2243+39	22 43 32.8	39 25 28	70	19	130	4.9	> 0.213	11
3C465	23 35 58.9	26 45 17	98	15	270	1.4	0.243	9
2354+14	23 54 44.9	14 29 28	-15	23	133	1.4	> 0.154	16

Lobe dominated quasar references:

1 Fanti (1986) A&AS 65 145
2 de Ruiter (1986) A&AS 65 111
3 Leahy and Williams (1984) MNRAS 210, 929
4 Fanti et al (1982) A&A 105, 200
5 Owen et al (1992) ApJSS 80 501
6 Owen et al (1993) ApJSS 87, 135
7 Baum (1987) Thesis
8 Burns et al (1983) ApJ 271 575
9 Leahy (1985) Thesis
10 Owen et al (1978) ApJL 226 L119
11 Riley et al MNRAS 80, 105
12 Riley and Pooley, MNRAS 183, 245
13 Laing, MNRAS 195, 261
14 Pooley and Henbest MNRAS 164, 271
15 Stocke et al (1982) IAU Symp 97, 39
16 Hintzen et al (1984) AJ 88, 709
17 Owen and Puschell (1984) AJ 89, 932
18 Taylor, G.B., et al (1990) ApJ 360, 41.
19 Condon and Broderick (1988) AJ 96, 30.
20 Burns, J.O., et al (1984) ApJ 283, 515.
21 Alexander and Leahy (1987) MNRAS 225, 1.

Figure 1: Estimated integrated source counts of flat spectrum quasars and steep spectrum quasar cores at 90 GHz.

Figure 2: Distribution of spectral index between 8.4 GHz and 90 GHz for flat spectrum quasars (FSQs) and steep spectrum quasars (SSQs).

Figure 3: Distribution of core fraction for flat spectrum quasars (FSQs) as calculated from Patnaik's data, and for the steep spectrum quasars (SSQs) as calculated from the steep spectrum subsample of the 3CRR sample.

Figure 4: Estimated integrated source counts at 30 GHz and 90 GHz.

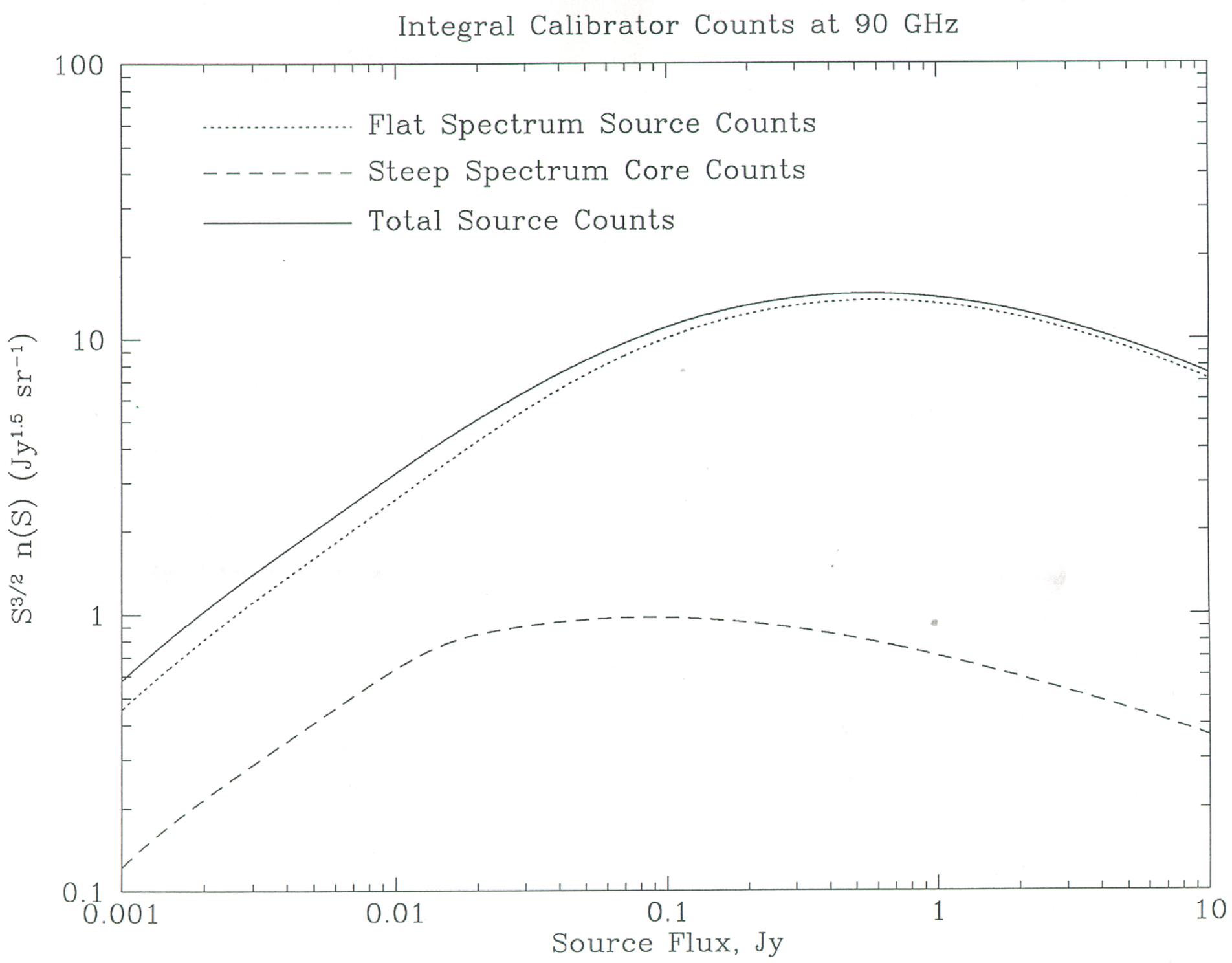
Integral Calibrator Counts at 90 GHz
Flat Spectrum Source Counts
Steep Spectrum Core Counts
Total Source Counts
100
10
1
0.1
$S^{3/2}$ n(S) ($Jy^{1.5}$ sr^{-1})
0.001
0.01
0.1
1
10
Source Flux, Jy

Figure 1

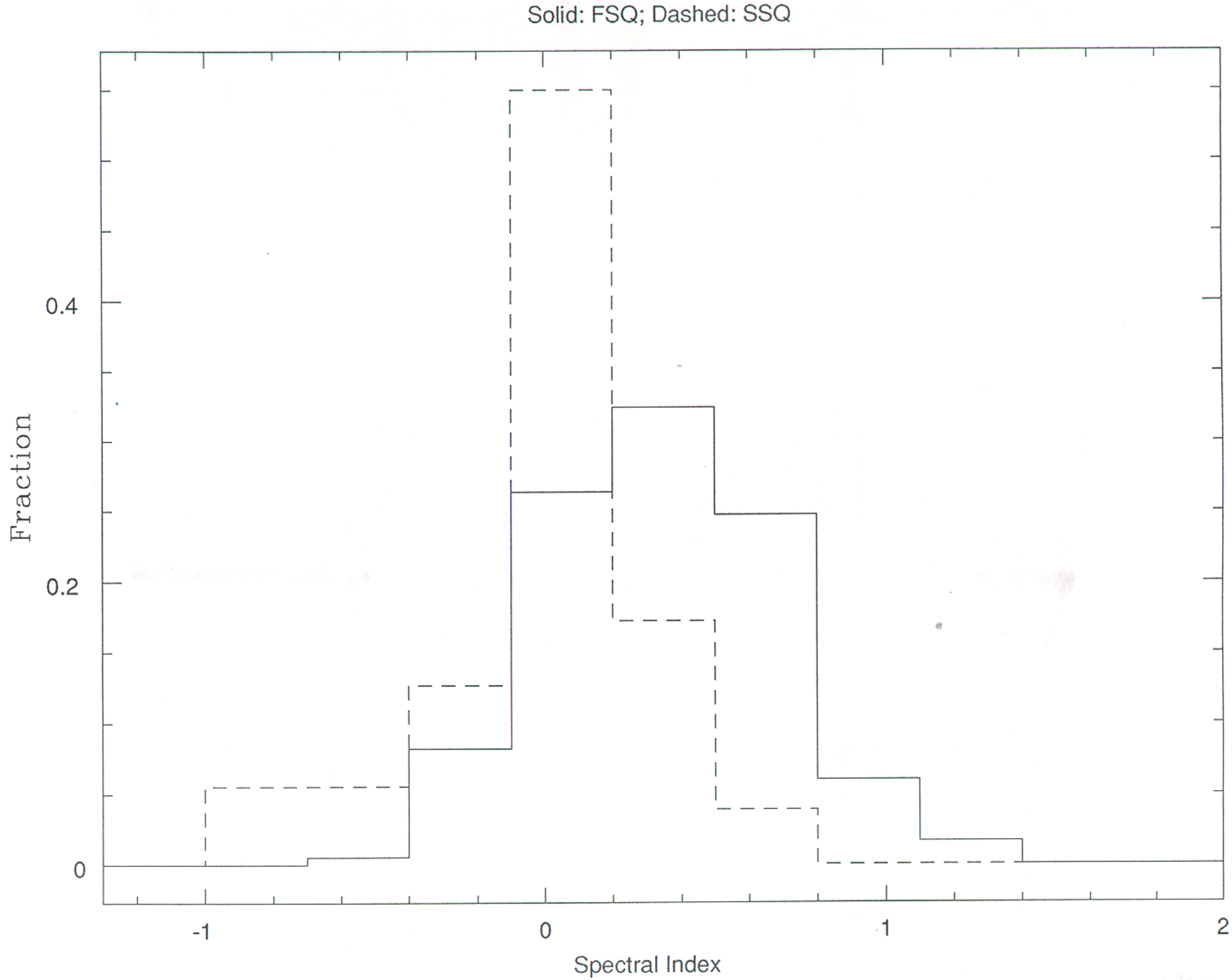

Figure 2

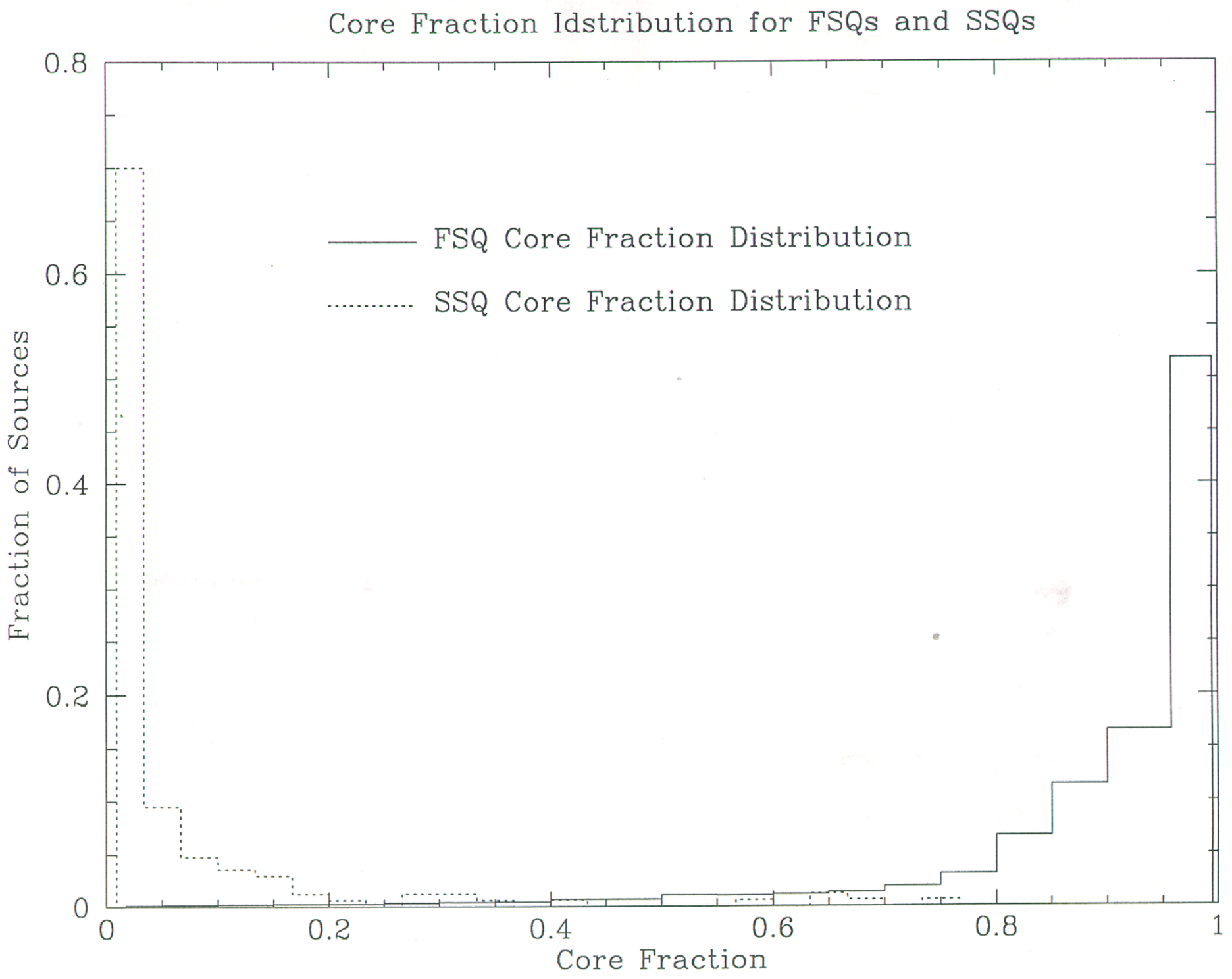
Core Fraction Idstribution for FSQs and SSQs
FSQ Core Fraction Distribution
SSQ Core Fraction Distribution
Fraction of Sources
Core Fraction
0
0.2
0.4
0.6
0.8
1

Figure 3

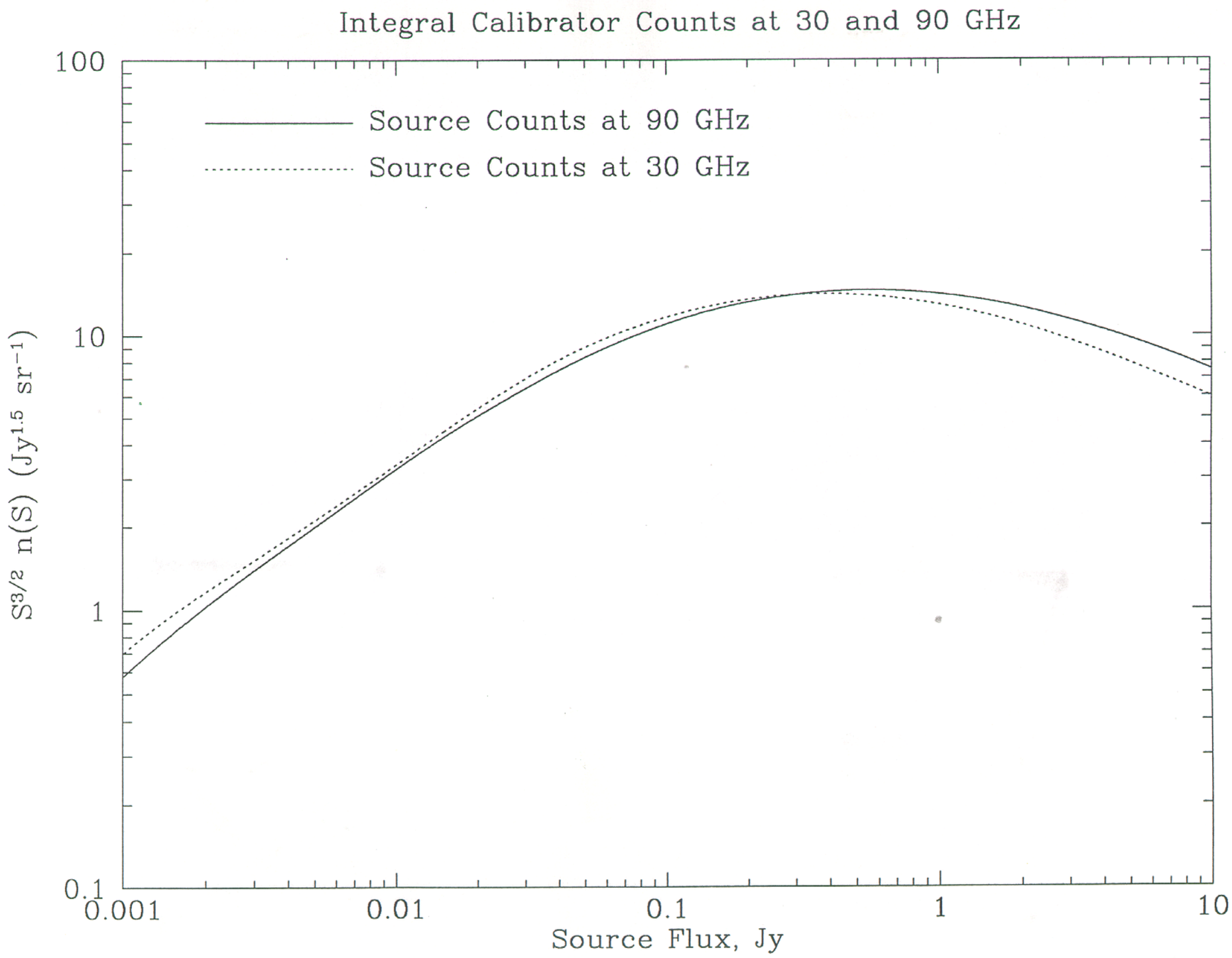
Integral Calibrator Counts at 30 and 90 GHz
Source Counts at 90 GHz
Source Counts at 30 GHz
100
10
1
0.1
0.001
0.01
0.1
1
10
S^3/2 n(S) (Jy^1.5 sr^-1)
Source Flux, Jy

Figure 4